Synthetic Peptide Models for the Redox-Active Disulfide Loop of Glutaredoxin. Conformational Studies†

R. Kishore,‡ S. Raghothama,§ and P. Balaram*,‡

Molecular Biophysics Unit and Sophisticated Instruments Facility, Indian Institute of Science, Bangalore 560 012, India

Received July 31, 1987; Revised Manuscript Received November 19, 1987

ABSTRACT: Two cyclic peptide disulfides Boc-Cys-Pro-X-Cys-NHMe (X = L-Tyr or L-Phe) have been synthesized as models for the 14-membered redox-active disulfide loop of glutaredoxin. ^{1}H NMR studies at 270 MHz in chloroform solutions establish a type I β-turn conformation for the Pro-X segment in both peptides, stabilized by a 4→1 hydrogen bond between the Cys(1) CO and Cys(4) NH groups. Nuclear Overhauser effects establish that the aromatic ring in the X = Phe peptide is oriented over the central peptide unit. In dimethyl sulfoxide solutions two conformational species are observed in slow exchange on the NMR time scale, for both peptides. These are assigned to type I and type II β-turn structures with -Pro-Tyr(Phe)- as the corner residues. The structural assignments are based on correlation of NMR parameters with model 14-membered cyclic cystine peptides with Pro-X spacers. Circular dichroism studies based on the –S–S– n–σ^* transition suggest a structural change in the disulfide bridge with changing solvent polarity, establishing conformational coupling between the peptide backbone and the disulfide linkage in these systems.

Redox-active disulfide loops in proteins can play an important role in thiol-dependent redox reactions (Holmgren, 1981, 1985) and in thiol–disulfide interchange processes (Ziegler, 1985; Meister & Anderson, 1983). Thioredoxins and glutaredoxins are small, heat-stable proteins with a 14-membered active site disulfide loop which participate in a variety of redox processes (Holmgren, 1981, 1986). The redox-active disulfide loops in these proteins are generated by disulfide bond formation between cysteine residues, which are separated by only two intervening amino acids in the primary structure. In the case of thioredoxins the intervening sequence is Gly-Pro [-Cys(32)-Gly-Pro-Cys(35)-][1] (Holmgren, 1968, 1985), while in case of glutaredoxins the intervening sequence is Pro-Tyr [-Cys(11)-Pro-Tyr-Cys(14)-] isolated from *Escherichia coli* (Hoog et al., 1984). The striking feature of thioredoxins and glutaredoxins is the presence of an invariant, 14-membered disulfide loop at the active site of these proteins which appears to be conserved during evolution (Holmgren, 1981; Klintrot et al., 1984; Hoog et al., 1984). The relatively small size of these disulfide loops suggests that there may be a relationship between the structural characteristics of these segments and their redox properties. There have been no detailed investigations on the conformational properties of these disulfide loops, although a 2.8-Å crystal structure is available for *E. coli* thioredoxin, in its oxidized form (Holmgren et al., 1975).

As part of a continuing program to investigate the structural properties of small ring peptide disulfides (Ravi & Balaram, 1983, 1984; Ravi et al., 1983; Venkatachalapathi et al., 1982) we describe in this report the conformational analysis of a synthetic peptide Boc-Cys-Pro-Tyr-Cys-NHCH$_3$ (**1**) corresponding to the active site disulfide loop of glutaredoxins. Studies on a model peptide Boc-Cys-Pro-Phe-Cys-NHCH$_3$ (**2**) are also presented, which serve to clarify specific spectral assignments.

Experimental Procedures

Synthesis of Peptides. Peptides **1** and **2** were synthesized by classical solution-phase procedures. The experimental protocols used were essentially similar to that described earlier (Ravi & Balaram, 1984; Venkatachalapathi et al., 1982) for related 14-membered cyclic disulfides. Detailed synthetic procedures and physical characterization of all the intermediate fragments are reported elsewhere (Kishore, 1985). Identity of these peptides was confirmed at every stage of synthesis by 60-, 80-, or 270-MHz ^{1}H NMR. Purification of peptide disulfides **1** and **2** was performed on a silica gel column using chloroform and 2–4% CH_3OH–$CHCl_3$ mixtures as eluents. The 14-membered disulfides **1** and **2** were obtained as white solids (cyclization yield **1** 14%, **2** 13%; mp **1** 166 °C, **2** 184 °C). Both peptides **1** and **2** were shown to be homogeneous by silica gel thin-layer chromatography and by high-performance liquid chromatography on a Lichrosorb RP-18 column (**1**, retention time 23.8 min, flow rate 0.6 mL min^{-1}, gradient 45–65% CH_3OH–H_2O in 30 min, filter 280 nm; **2**, retention time 25.1 min, flow rate 0.8 mL min^{-1}, gradient 45–65% CH_3OH–H_2O in 20 min, filter 226 nm). The monomeric structure of peptide disulfides **1** and **2** was confirmed by observation of a molecular ion peak in the fast atom bombardment mass spectrum (**1**, MH^+ = 596; **2**, MH^+ = 580). Peptides **1** and **2** were fully characterized by 270-MHz ^{1}H and 67.89-MHz ^{13}C NMR. Representative data of peptide **1** are shown in Figure 1.

Spectroscopic Methods. All NMR studies were carried out on a Bruker WH-270 FT-NMR spectrometer as described

† Supported by a grant from the Department of Science and Technology, Government of India.

* Correspondence should be addressed to this author.
‡ Molecular Biophysics Unit.
§ Sophisticated Instruments Facility.

[1] Abbreviations: Aib, α-aminoisobutyric acid; CD, circular dichroism; FT, Fourier transform; TMS, tetramethylsilane; COSY, correlated spectroscopy; TEMPO, 2,2,6,6-tetramethylpiperidinyl-1-oxy; TMP, trimethyl phosphate; Piv, pivaloyl. The abbreviations used for amino acids, peptides, and protecting groups are those recommended by the IUPAC–IUB Commission on Biochemical Nomenclature.

0006-2960/88/0427-2462$01.50/0

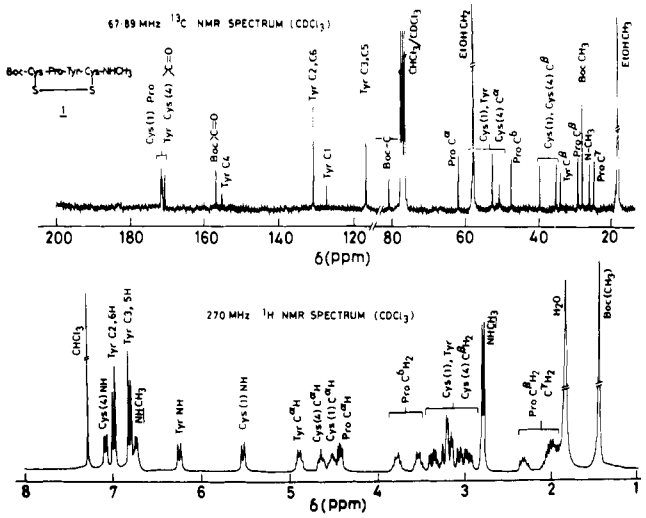

FIGURE 1: ^{1}H and ^{13}C NMR spectra of peptide **1** in $CDCl_3$.

earlier (Rao et al., 1983). Infrared (IR) spectra were recorded on a Perkin-Elmer Model 297 spectrometer using a path length of 4 mm, in dry $CHCl_3$ solutions. Circular dichroism (CD) measurements were performed by using a Jasco J-20 spectropolarimeter. Measurements in the 210–240-nm range were carried out by using 1-mm path length cells, while cells of path length 5 mm were used in the 240–340-nm range. Peptide concentrations were maintained at 1 mg mL^{-1}, and reported values are expressed as molar ellipticity ($[\theta]_M$) in deg cm^2 dmol^{-1}.

Results and Discussion

NMR Studies. Extremely well resolved NMR spectra were obtained at ambient temperature for both peptides **1** and **2** in $CDCl_3$ (cf. Figure 1). The resonance assignments are based on spin-decoupling experiments. The Cys(1) spin system may be readily identified since the urethane resonance appears at higher field (5.27–5.29 ppm) in $CDCl_3$ (Ravi & Balaram, 1983, 1984; Bystrov et al., 1965). Unequivocal assignments of the spin system for Cys(4) and Tyr/Phe residues in these peptides is rendered difficult by extensive overlap of the $C^\beta H_2$ resonances of the cysteine and aromatic residues (2.5–3.0 ppm) (Wüthrich, 1976). However, in several related sequences the $C^\alpha H$ resonances of the Tyr/Phe residues occur at lower field (4.90–4.98 ppm) than the Cys $C^\alpha H$ resonances. Furthermore, in a large number of 14-membered cyclic peptide disulfides, containing -Pro-L-X-intervening sequences, the Cys(4) NH resonances occur at low field in $CDCl_3$ (~7.2 ppm), while the X residue NH group appears at significantly higher field (~6.3 ppm) (Ravi & Balaram, 1984). Therefore, the Cys(4) NH in peptides **1** and **2** is assigned to the doublet at 7.03 and 7.02 ppm, respectively. The Tyr and Phe NH groups are assigned to the resonances at 6.15 and 6.10 ppm in peptides **1** and **2**, respectively.

The ^{1}H NMR spectra of peptide **1** in $(CD_3)_2SO$ solution are shown in Figure 2 (data not shown for peptide **2**). It is clear from the spectra that at 293 K in $(CD_3)_2SO$ the peptides exist as two distinct species, major (M) and minor (m), in slow exchange on the NMR time scale. Evaporation of $(CD_3)_2SO$ followed by redissolution in $CDCl_3$ resulted in the observation of only a single species, suggesting that the process observed in $(CD_3)_2SO$ is completely reversible. This experiment eliminates the possibility of an irreversible structural transition occurring in $(CD_3)_2SO$. Solid-state infrared studies of peptide samples obtained by evaporation of $CDCl_3$ and $(CD_3)_2SO$ confirmed the absence of any degradative effect in $(CD_3)_2SO$.

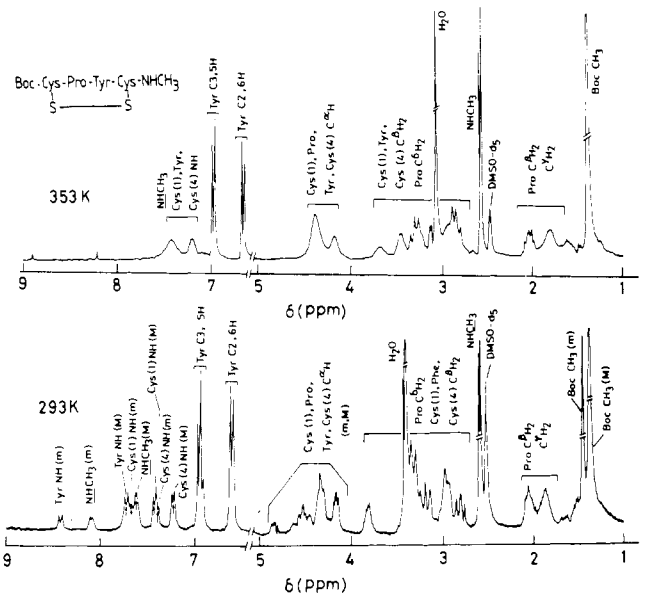

FIGURE 2: 270-MHz ^{1}H NMR spectra of peptide **1** in $(CD_3)_2SO$. Temperatures are indicated against each spectrum. Note the coalescence of NH and $C^\alpha H$ resonances at 353 K. Major (M) and minor (m) NH resonances are marked.

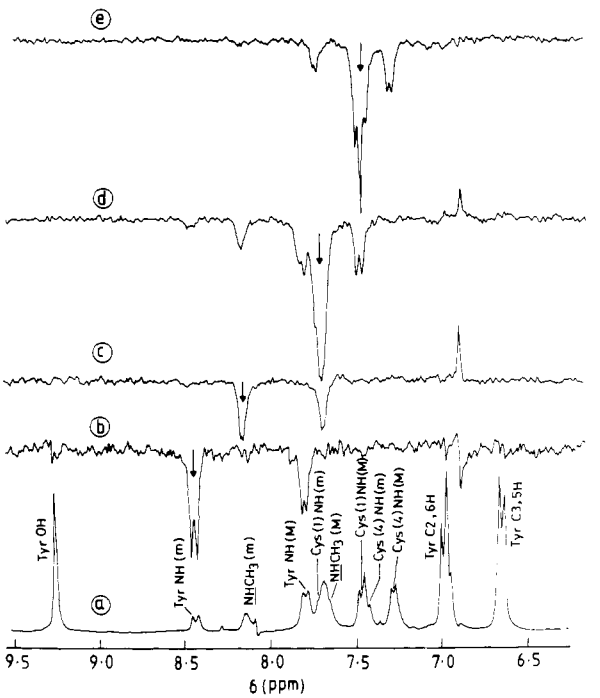

FIGURE 3: (a) Partial 270-MHz ^{1}H NMR spectra of peptide **1** in $(CD_3)_2SO$. (b–e) Difference spectra recorded after saturating specific NH resonances, indicated by arrows. Major (M) and minor (m) resonances are marked.

At 353 K (Figure 2) the major and minor spectra interconvert rapidly and chemical shift averaging is observed.

Solvent titration experiments in $CDCl_3$–$(CD_3)_2SO$ mixtures establish that the major (M) conformer in $(CD_3)_2SO$ corresponds to the only conformation observed in $CDCl_3$. Assignments of the various NH resonances in conformer M were then established by monitoring the changes in NH chemical shifts, in $CDCl_3$–$(CD_3)_2SO$ mixtures of varying compositions. The NH resonances of the minor (m) conformer in peptides **1** and **2** were established by a double-resonance experiment involving transfer of saturation by chemical exchange (Hoffmann & Forsen, 1966). Figure 3 illustrates a representative transfer of saturation experiments carried out on

Table I: 270-MHz ^{1}H NMR Parameters[a] for Peptides **1** and **2**

parameters	X = L-Tyr (**1**), for residue				X = L-Phe (**2**), for residue			
	Cys(1)	Tyr	Cys(4)	*NH*CH_3	Cys(1)	Phe	Cys(4)	*NH*CH_3
$\delta_{NH}(CDCl_3)$	5.27	6.15	7.03	6.54	5.19	6.10	7.02	6.50
$\delta_{C^\alpha H}(CDCl_3)$	4.50	4.90	4.63		4.51	4.99	4.67	
$\delta_{NH}[(CD_3)_2SO]$ (M)	7.48	7.78	7.28	7.67	7.48	7.86	7.26[e]	7.70
$\delta_{NH}[(CD_3)_2SO]$ (m)	7.73	8.45	7.44	8.13	7.74	8.49	7.44	8.14
$\delta_{C^\alpha H}[(CD_3)_2SO]$ (M)	4.46	4.26	4.25	4.08	*g*	*g*	*g*	*g*
$\delta_{C^\alpha H}[(CD_3)_2SO]$ (m)	4.15	4.51	4.77		*g*	*g*	*g*	*g*
$^3J_{HNC^\alpha H}(CDCl_3)$[b]	9.5	9.5	8.1		8.8	9.5	8.1	
$^3J_{HNC^\alpha H}[(CD_3)_2SO]$ (M)[b]	8.8	8.8	6.6		8.8	8.1	*f*	
$^3J_{HNC^\alpha H}[(CD_3)_2SO]$ (m)[b]	7.3	9.5	*f*		6.0	8.8	7.6	
$\Delta\delta_{NH}$ (M)[c]	2.21	1.63	0.25	1.13	2.29	1.76	0.24	1.20
$d\delta/dT$ (M)[d]	0.0065	0.0060	0.0013	0.0041	0.0066	0.0063	*f*	0.0035
$d\delta/dT$ (m)[d]	0.0055	0.0012	0.0014	0.0051	0.0043	0.0015	0.0008	0.0055

[a] δ values are expressed as ppm downfield from internal TMS and are reported for peptide concentrations of ~6 and 12 mM in $CDCl_3$ and $(CD_3)_2SO$ for peptide **1** and 16 mM in both solvents for peptide **2**. Pro $C^\alpha H$ resonance appears at 4.42 ppm in both peptides. [b] Errors in J values are ±0.4 Hz. [c] $\Delta\delta_{NH} = \delta_{NH}[(CD_3)_2SO]$ (M) − $\delta_{NH}(CDCl_3)$. [d] $d\delta/dT$ values are determined in $(CD_3)_2SO$ and expressed as ppm/K. (M) and (m) indicate major and minor conformers, respectively, observed in $(CD_3)_2SO$. [e] δ_{NH} value is determined from the transfer of saturation experiment. [f] Values could not be determined due to spectral overlaps. [g] COSY spectra were not obtained for **2**.

peptide **1** which permits the assignments of the NH resonances of the m conformer in $(CD_3)_2SO$. It may be noted that irradiation of closely overlapping resonances leads to saturation transfer to more than one peak. The assignments of $C^\alpha H$ resonances of M and m conformers were made by using NH ↔ $C^\alpha H$ connectivities in a two-dimensional COSY spectrum (Bax & Lerner, 1986). The relevant NMR parameters for both peptides are summarized in Table I.

Conformational Studies in Chloroform Solution. Delineation of Hydrogen-Bonded NH Groups in $CDCl_3$. The presence of solvent-shielded or intramolecularly hydrogen bonded NH groups was established by using the following criteria: (i) solvent dependence of NH chemical shifts in $CDCl_3$–$(CD_3)_2SO$ mixtures, (ii) nitroxide radical induced line broadening of NH resonances, and (iii) rates of hydrogen–deuterium (H–D) exchange in $CDCl_3$–D_2O mixtures (Wüthrich, 1976; Balaram, 1985).

In both peptides **1** and **2**, the Cys(1) NH group moves rapidly downfield on increasing $(CD_3)_2SO$ concentrations, in $CDCl_3$–$(CD_3)_2SO$ mixtures (results not shown), while the Cys(4) NH shows only very small shifts, under similar conditions. The methylamide and Tyr/Phe NH groups exhibit an intermediate downfield shift on increasing $(CD_3)_2SO$ concentrations. The solvent shift values $\Delta\delta$ of NH groups in both peptides **1** and **2** are summarized in Table I. A large $\Delta\delta$ (>2.2 ppm) value for Cys(1) NH suggests that the NH group is solvent exposed in both peptides. In both peptides the $\Delta\delta$ value for the Cys(4) NH is very small (<0.24 ppm), suggesting that the Cys(4) NH group is strongly solvent shielded in both cases. Intermediate $\Delta\delta$ values (~1.13–1.77 ppm) have been observed for the methylamide and Tyr/Phe NH groups, suggesting that these NH groups are partly solvent shielded. However, the methylamide NH groups are relatively more solvent shielded than the Tyr/Phe NH groups, in both peptides.

Further evidence for the solvent-shielded nature of NH groups in these two peptides was also obtained from radical-induced line broadening of NH resonances in $CDCl_3$ (results not shown). The extent of line broadening follows the order Cys(1) NH ≫ methylamide NH ~ Tyr NH ~ Cys(4) NH for peptide **1** and Cys(1) NH > Phe NH > methylamide NH > Cys(4) NH for peptide **2**. These results strongly suggest that, in $CDCl_3$, the Cys(1) NH is solvent exposed, whereas the Cys(4) NH is strongly solvent shielded, presumably by involvement in intramolecular hydrogen bonding, in both peptides. An interesting feature of this experiment is that the extent of line broadening for the Phe NH in peptide **2** is considerably more than that for the corresponding Tyr NH in peptide **1**. This is presumably a result of hydrogen bonding of the radical to the phenolic OH, which should sterically impede further interaction of another TEMPO molecule with the Tyr NH group. However, the Phe NH resonance exhibits an intermediate line broadening, suggesting that this NH group is partly solvent exposed. In both peptides, the extent of line broadening for the methylamide NH proton is rather low, suggesting that the C-terminal NH group is partly shielded from the solvent.

Hydrogen–deuterium (H–D) exchange experiments in $CDCl_3$–D_2O mixtures have also been carried out to delineate the solvent-shielded NH groups in $CDCl_3$ (data not shown). The use of heterogeneous solvent systems precludes comparison between the two peptides. No attempt has been made to quantitate the H–D exchange data, since a qualitative ordering of NH groups is sufficient for delineating solvent-shielded NH protons. In these experiments, the Cys(1) NH proton exchanged very rapidly. However, the remaining NH protons exchange rather slowly in both peptides, suggesting their relative inaccessibility to the solvent.

IR Studies. Evidence for the presence of intramolecular hydrogen-bonded conformation was obtained from IR studies in $CHCl_3$ solution. IR spectra of the two peptides **1** and **2** in $CHCl_3$ exhibit two intense NH stretching bands at ν_{NH} 3380–3370 cm^{-1} and ν_{NH} 3450–3440 cm^{-1}, corresponding to both hydrogen-bonded [ν_{NH}(hb)] and free [ν_{NH}(f)] NH groups, respectively. The relative intensities of ν_{NH}(hb) and ν_{NH}(f) remained unchanged up to a concentration of 1 mM, suggesting that intramolecular hydrogen bonds do contribute to this absorption band. Earlier IR studies on several other 14-membered cyclic peptide disulfides having Pro-X intervening sequences have yielded similar results (Venkatachalapathi et al., 1982; Ravi & Balaram, 1984).

*Hydrogen-Bonded Structures of Peptides **1** and **2** in Chloroform.* In chloroform solution a single species is observed by ^{1}H NMR in both peptides **1** and **2**. ^{13}C NMR spectra at 67.89 MHz of peptides **1** and **2** show that the positions of Pro C^β (29.5 ppm) and Pro C^γ (25.0 ppm) are characteristic of trans X-Pro peptide bonds (Wüthrich, 1976). Therefore, only conformations with an all-trans peptide backbone need to be considered for these Pro-Tyr/Phe-containing sequences.

The NMR results suggest that the Cys(4) NH is intramolecularly hydrogen bonded in both peptides while the Cys(1) NH is fully exposed to the solvent. The remaining two NH groups (methylamide NH and Tyr/Phe NH) appear to show a moderate degree of shielding from the solvent. Earlier

Table II: 270-MHz NOE Data[a] on Peptide Disulfides **1** and **2** in $CDCl_3$

X = L-Phe (**2**)			X = L-Tyr (**1**)		
resonance irradiated	NOE observed	% enhancement	resonance irradiated	NOE observed	% enhancement
Phe C2H, C5H	Phe NH	5.1	Cys(4) NH	Tyr NH	5.5
	Pro H_1^β	4.2		Cys(4) $C^\alpha H$	5.0
Cys(4) NH	Phe NH	8.2	$NHCH_3$	$NHCH_3$	2.7
	Phe $C^\alpha H$	4.9	Tyr NH	Cys(4) NH	4.7
	Cys(4) $C^\alpha H$	5.8		Tyr $C^\alpha H$	5.0
$NHCH_3$	Cys(4) $C^\alpha H$	5.0		Tyr 2,6H	2.0
	$NHCH_3$	3.5		Tyr 3,5H	2.1
Phe NH	Phe C2H, C5H	2.8	Pro H_1^β	Pro $C^\alpha H$	11.6
	Cys(4) NH	7.2		Pro H_1^γ, H_2^γ, H_2^β[b]	3.6
	Phe $C^\alpha H$	4.9	Pro H_2^β, H_1^γ, H_2^γ[b]	Pro H_1^β	11.5
	Pro $C^\alpha H$	2.0		Tyr 2,6H	1.3
Cys(4) $C^\alpha H$	$NHCH_3$	2.3		Tyr 3,5H	1.4
Cys(1) $C^\alpha H$	Pro H_1^δ	5.6			
	Pro H_2^δ	3.1			
	Cys(1) NH	2.3			
Pro $C^\alpha H$	Pro H_1^β	6.3			
Pro H_1^β	Pro H_2^β, H_2^γ[b]	7.6			
	Pro $C^\alpha H$	12.0			
Pro H_1^γ	Pro H_1^β	4.2			
	Pro H_1^δ	4.5			
Pro, H_2^β, H_2^γ[b]	Pro H_1^β	14.8			
	Pro $C^\alpha H$	5.0			
	Pro H_2^δ	4.2			
	Phe NH	2.4			
	Phe C2H, C5H	1.3			

[a] NOE experiments were carried out at a probe temperature of 293 K and were reported for a peptide concentration of ~6 and 35 mM for peptides **1** and **2**, respectively. [b] Pro H_2^β, H_1^γ, and H_2^γ resonances in **1** and Pro H_2^β and H_2^γ in **2** are overlapping. No appreciable NOEs were detected when the Cys(1) NH, Cys(1) $C^\alpha H$, Cys(4) $C^\alpha H$, Pro $C^\alpha H$, Tyr $C^\alpha H$, Tyr 2,6H and Tyr 3,5H resonances were irradiated.

studies on 14-membered cyclic peptide disulfides having Pro-X (X = Ala, Gly, Leu, Val, Aib, D-Ala) sequences, as spacer residues, have clearly established the stabilization of Pro-X β-turns in these cases, involving a transannular 4→1 hydrogen bond between the Cys(1) CO and Cys(4) NH groups (Venkatachalapathi, 1982; Ravi & Balaram, 1984; Ravi et al., 1983; Rao et al., 1983). The NMR results for peptides **1** and **2** are fully compatible with Pro-Tyr/Phe β-turn conformations, stabilized by a 4→1 hydrogen bond, as illustrated in Figure 4a. For Pro-L-X sequences type I (III) conformations ($\phi_{i+1} \sim -60°$, $\psi_{i+1} \sim -30°$, and $\phi_{i+2} \sim -90°$, $\psi_{i+2} \sim 0°$) are likely to be favored (Balaram, 1984; Smith & Pease, 1980; Zimmerman & Scheraga, 1977; Prasad & Balaram, 1984; Rose et al., 1985). However, type II structures ($\phi_{i+1} \sim -60°$, $\psi_{i+1} \sim +120°$, and $\phi_{i+2} \sim +80°$, $\psi_{i+2} \sim 0°$) cannot be strictly excluded. Indeed L residues have been observed at the $i + 2$ position of type II β-turns, albeit infrequently. An unambiguous distinction between type I and type II conformations may be made from nuclear Overhauser effect (NOE) studies. In a type II β-turn conformation a significant NOE is observed between the $C^\alpha_{i+1}H$ and $N_{i+2}H$ protons.

NOE Studies on Peptides **1** *and* **2** *in* $CDCl_3$. Difference NOE experiments have been carried out at 270 MHz in $CDCl_3$, for both peptides **1** and **2** at 293 K. Peptide concentrations employed were ~6 mM for **1** and ~35 mM for **2**. All observed NOEs, under these conditions, are positive, suggesting that the peptides' rotational correlation times are short enough to be in the region $\omega\tau_c < 1$. Representative difference NOE spectra obtained for peptide **2** are shown in Figure 5. The results of these studies for both peptides are summarized in Table II.

In peptide **2** irradiation of the Phe NH proton results in a large NOE on the Cys(4) NH proton (7.2%) (Figure 5b). In addition, a direct intraresidue NOE on the Phe $C^\alpha H$ proton (4.9%) and weak NOEs on the aromatic ring C2H and C5H (2.8%) are also observed (Figure 5b). A very weak effect of ~2% is observed at the Pro $C^\alpha H$. These results suggest that type I β-turn conformations are significantly populated, since

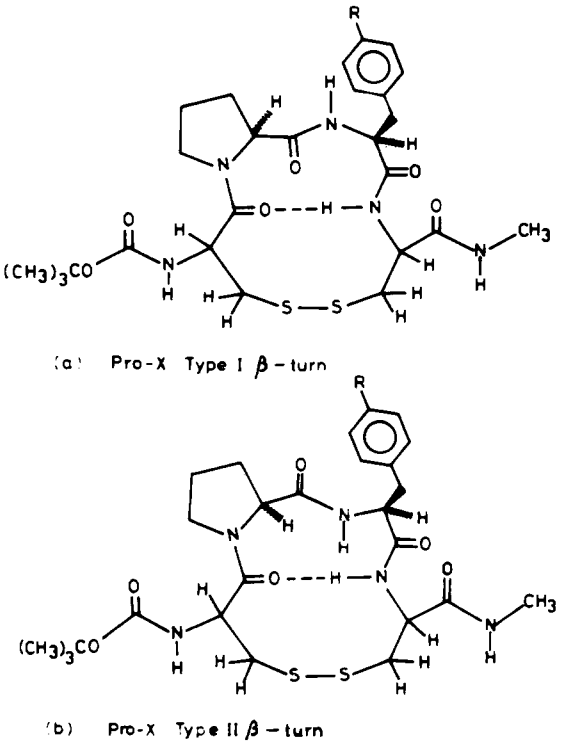

FIGURE 4: Schematic representation of the β-turn conformations proposed for peptides **1** and **2**. (Top) Pro-X (X = Tyr or Phe) type I β-turn in $CDCl_3$ and $(CD_3)_2SO$, major (M) conformer. (Bottom) Pro-X type II β-turn in $(CD_3)_2SO$ minor conformer [R = OH, Tyr (**1**); R = H, Phe (**2**)].

a substantial NOE is not observed between Phe NH and Pro $C^\alpha H$. The observation of a large NOE between the Phe NH and Cys(4) NH groups (Figures 5b,c) is consistent with a type I (III) conformation where the interproton distance, $N_{i+2}H \leftrightarrow N_{i+3}H$, is estimated to be ~2.4 Å (Wüthrich et al., 1984). The observation of NOEs between the aromatic C2H and C5H protons and the Phe NH is consistent with conformations

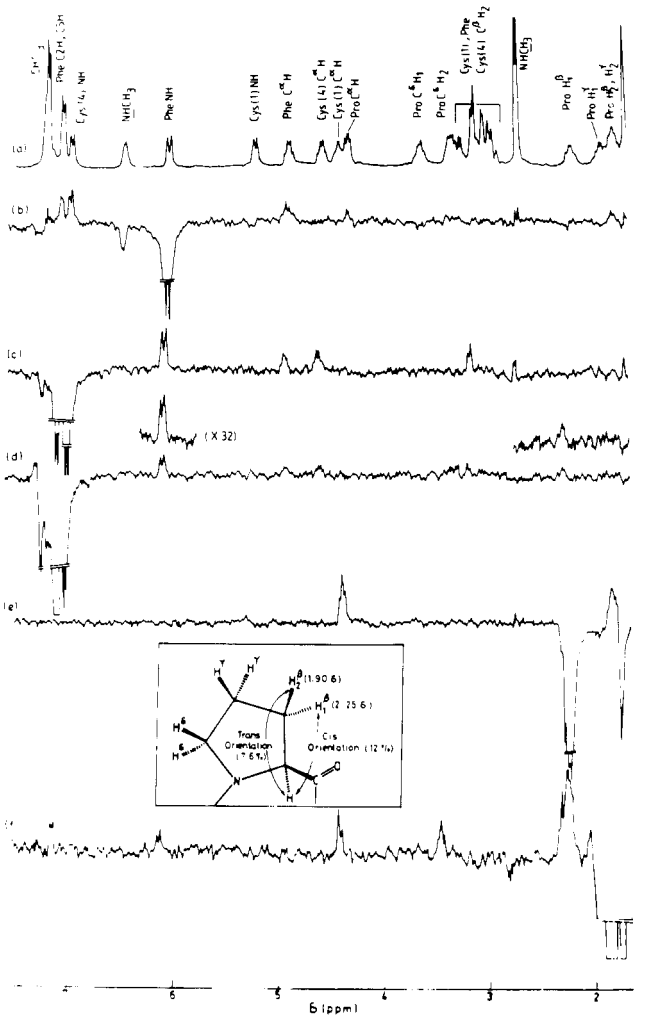

FIGURE 5: (a) 270-MHz ^{1}H NMR spectrum of peptide **2** in $CDCl_3$ at 293 K. (b–f) Difference NOE spectra recorded by irradiation of (b) Phe NH; (c) Cys(4) NH; (d) Phe C2H, C5H; (e) Pro H^{β}_1; and (f) Pro H^{γ} and Pro H^{β}_2, H^{γ}_2. The difference spectra were obtained by subtracting normal spectra, with the irradiation frequency offset, from perturbed spectra, where the irradiating frequency saturates a specific resonance. Typically, 200 accumulations were used in each case, with a delay time of 3 s between transients. The spectra are magnified by a factor of 16 or 32 as indicated. In the case of weak NOEs magnification by a factor of 32 is also shown. Peptide concentration was ~35 mM.

that orient the aromatic ring over the central peptide unit of the β-turn.

Theoretical conformational energy calculations suggest that, in the model dipeptide Ac-Pro-Phe-$NHCH_3$, both type I and type II β-turn structures are in fact energetically favorable (P. K. C. Paul, unpublished results). Further, in both types of β-turns there are low-energy conformations that orient the aromatic ring above the central peptide unit, linking the Pro and Phe residues. Low-energy conformations also exist in which the aromatic ring orients above the peptide unit linking the Phe and terminal amide unit [i.e., this corresponds to the peptide bond between Tyr(3)/Phe(3) and Cys(4) residues in **1** and **2**]. Figure 6 illustrates the perspective diagrams of the low-energy conformations computed for the Ac-Pro-Phe-$NHCH_3$ sequence. In conformations that place the aromatic ring above the central peptide unit, close approach of the Phe C2H and C5H aromatic protons to the Phe NH group is possible. This is consistent with the NOE of 5.1% observed on the Phe NH proton when the Phe C2H and C5H protons (~7.13 ppm) are irradiated (Figure 5d). The Pro $C^{\beta}H_2$ protons appear as complex multiplets centered at ~2.25 and

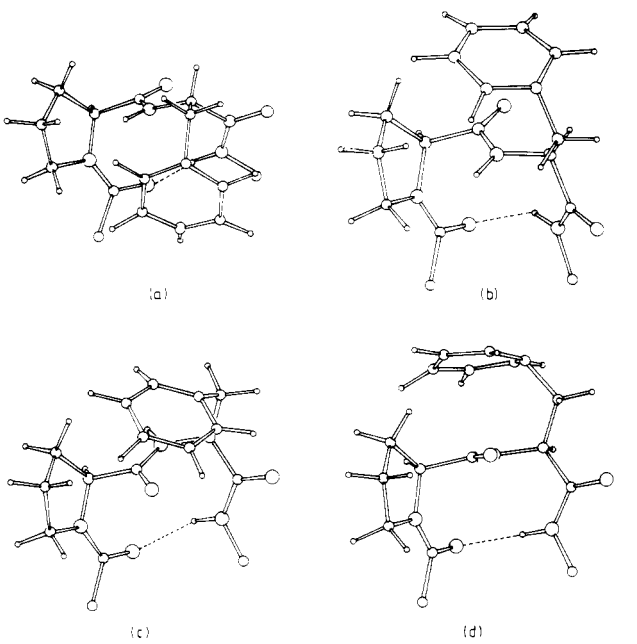

FIGURE 6: Perspective diagrams of the low-energy conformations computed for Ac-Pro-Phe-$NHCH_3$. A 4→1 hydrogen bond is indicated by dotted line. (a) and (b) correspond to type I β-turns; (c) and (d) correspond to type II β-turns.

~1.90 ppm while the Pro $C^{\gamma}H_2$ protons appear as multiplets centered at ~2.0 and ~1.90 ppm. It may be noted that the resonances of Pro H^{β}_2 and Pro H^{γ} overlap. The Pro H^{δ}_1 and Pro H^{δ}_2 protons appear as multiplets at ~3.7 and ~3.45 ppm, respectively. Irradiation of the low-field Pro H^{β}_1 results in a 12% NOE on the Pro $C^{\alpha}H$ (Figure 5e) proton, confirming their cis orientation. This permits assignment of the resonance at ~1.90 ppm to the Pro H^{β}_2 proton which will be oriented in a trans fashion to the Pro $C^{\alpha}H$ proton.

Irradiation of the upfield Pro H^{β}_2 resonance results in the observation of weak NOEs at the C2H and C5H aromatic protons (1.3%) and the Phe NH proton (2.4%) (see Figure 5f). The observation of these NOEs suggests that conformers involving a close approach of the aromatic side chain to the Pro residue and the central peptide unit are, indeed, populated. It may be noted that the other NOEs observed in Figure 5f correspond to the Pro H^{β}_1 (geminal NOE), H^{δ}_2 (due to irradiation of the overlapping Pro H^{γ}_2 protons), and Pro $C^{\alpha}H$ proton. Note that this trans vicinal NOE (5%) is significantly less than the stronger cis vicinal NOE observed when Pro H^{β}_1 is irradiated (12%).

It is of particular interest to note that an NOE of 5% is observed on the Cys(4) $C^{\alpha}H$ proton, when the methylamide NH resonance is saturated (see Table II). Such an interresidue NOE ($C^{\alpha}_iH \leftrightarrow N_{i+1}H$) is observable only for Cys(4) ψ values of ~+120 ± 30°. The observation of this NOE would thus suggest that a second β-turn involving Phe(3) and Cys(4) as corner residues is unlikely, since such a structure would necessarily require Cys(4) ψ values of ~0°.

In the case of peptide **1** no detectable NOE was observed between the Tyr NH and Pro $C^{\alpha}H$ protons. A significant NOE was observed between Tyr NH and Cys(4) NH protons (Table II). These results suggest that the type I β-turn conformation at the Pro-Tyr segment is indeed favored. In peptide **1**, several of the NOEs observed in the case of **2** were absent or of extremely small magnitude. For example, no NOE was detected between the methylamide NH and the Cys(4) $C^{\alpha}H$ resonances. Further, only very weak NOEs were detected between the aromatic Tyr ring protons and the Pro $C^{\beta}H_2$ and

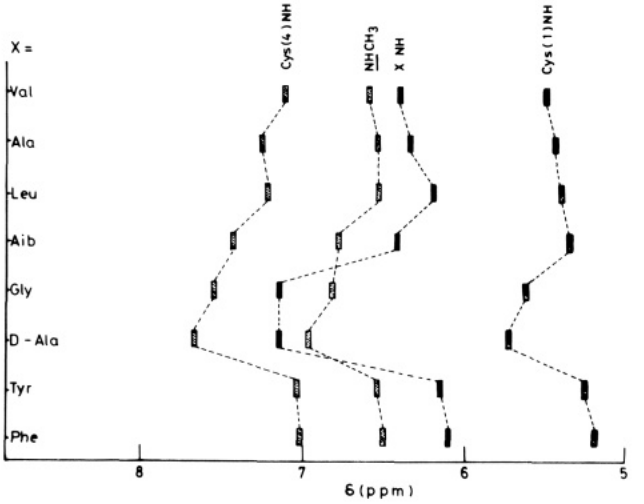

FIGURE 7: Schematic representation of chemical shifts of the NH resonances, in $CDCl_3$, in eight 14-membered cyclic peptide disulfides with Pro-X intervening sequences.

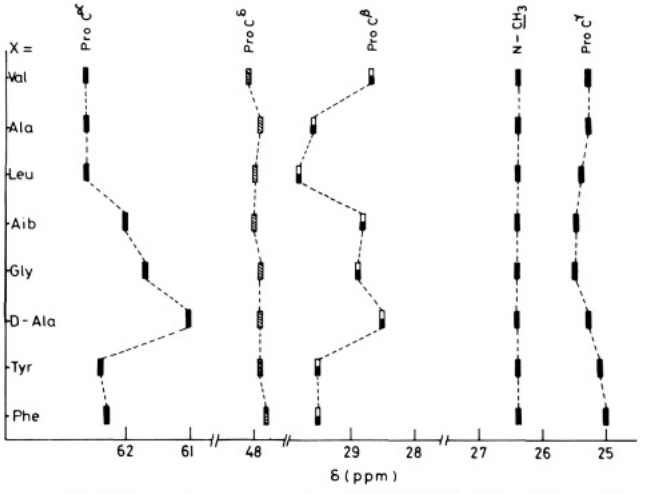

FIGURE 8: Schematic representation of ^{13}C NMR shifts of the proline ring, in $CDCl_3$, in eight 14-membered cyclic peptide disulfides with Pro-X intervening sequences.

Tyr NH protons (Table II). It is possible that in **1** the occurrence of other rotamers about the Tyr(3) χ^1 (C^α–C^β) bond results in different orientations of the aromatic ring as compared to peptide **2**.

Proposed Conformation of Peptides **1** *and* **2** *in Chloroform.* Earlier studies of Cys-Pro-X-Cys disulfide sequences have clearly established that type I, II, and III β-turn conformations can in fact be accommodated within 14-membered disulfide loops. While type I (III) conformations are favored for L residues at the $i + 2$ position (X = L-Ala, L-Leu, L-Val) of a β-turn, type II conformations have been suggested for X = D-Ala or Gly at the $i + 2$ position. For the achiral, hindered Aib residue, solvent-dependent equilibria between type I and type II β-turn structures have been observed (Ravi et al., 1983; Rao et al., 1983). The $N_{i+2}H$ (X NH) proton and the $N_{i+3}H$ [Cys(4) NH] proton should experience entirely different chemical environments in type I (III) and type II β-turn conformations. Figure 7 schematically compares the chemical shifts of the NH protons in $CDCl_3$ in eight 14-membered cyclic peptide disulfides with Pro-X intervening sequences. It is clearly seen that the peptides favoring type II β-turn conformations (X = D-Ala, Gly) have significantly lower field resonances for Cys(4) and X NH groups as compared to type I β-turn peptides. A similar chemical shift correlation for the ^{13}C resonances of the proline ring is given in Figure 8. The Pro C^α and Pro C^β resonances appear most sensitive to changes in the value of Pro ψ. High-field Pro C^α and Pro C^β resonances appear characteristic of type II β-turn conformations. The chemical shift correlation diagrams shown in Figures 7 and 8 provide convincing support for the conclusion that the peptides **1** and **2** favor a type I β-turn conformation in $CDCl_3$. As already noted, NOE studies also support type I β-turn conformations for peptides **1** and **2**. Studies of the NH resonance NMR parameters suggest the inaccessibility of the Cys(4) NH group to the solvent, supporting its involvement in an intramolecular hydrogen bond.

In earlier studies of 14-membered cyclic disulfides, it has been established that the formation of a Pro(2)-X(3) type I (III) β-turn often results in formation of a second, consecutive, X(3)-Cys(4) β-turn involving a 4→1 hydrogen bond between the Pro(2) CO and methylamide NH groups. Such consecutive β-turn structures have in fact been observed in the solid state in peptides with Pro-Aib (Ravi et al., 1983) and Pro-Leu (Balaram, 1984) intervening sequences. In the case of peptides **1** and **2** it appears that the methylamide NH group is not involved in a strong intramolecular hydrogen bond in chloroform solution. Peptides **1** and **2** would therefore appear to favor a single type I β-turn conformation of the type that has been established in the case of the -Pro-Val- sequence (Venkatachalapathi et al., 1982). A partial shielding of the X NH from the solvent may arise by appropriate orientation of the X residue side chain. This may account for the moderate degree of solvent shielding observed for the X NH protons in peptides **1** and **2**.

Conformational Studies in Dimethyl Sulfoxide. The 270-MHz ^1H NMR spectrum of peptide **1** in $(CD_3)_2SO$ is shown in Figure 2. It is evident from the spectra that in $(CD_3)_2SO$ the peptides **1** and **2** (data not shown for peptide **2**) exist as two distinct species, major (M) ~70% and minor (m) ~30%, in slow exchange on the NMR time scale. At 293 K sharp resonances are observed for both species in peptides **1** and **2**. Coalescence can be observed for both peptides **1** and **2**, on heating to ~353 K in $(CD_3)_2SO$. The representative 270-MHz ^1H NMR spectrum of peptide **1** observed at 353 K in $(CD_3)_2SO$ is illustrated in Figure 2.

As discussed in the preceding sections, assignments of various NH resonances in the m conformations may be made by establishing their connectivities to the corresponding NH resonances in the M conformations by transfer of saturation experiments (Figure 3). The fact that the M conformation in $(CD_3)_2SO$ corresponds to the species in $CDCl_3$ is established by solvent titration experiments in $CDCl_3$–$(CD_3)_2SO$ mixtures. The various NMR parameters, for both M and m for peptides **1** and **2** in $(CD_3)_2SO$, are summarized in Table I. The low temperature coefficient ($d\delta/dT$) values for the Cys(4) NH group suggest that this NH group is solvent shielded in both conformers. The Cys(1) and methylamide NH groups appear to be largely solvent exposed in both conformers, in peptides **1** and **2**. The Tyr/Phe NH group in both peptides appears to be solvent exposed in the major conformation and solvent shielded in the minor conformation. The NMR data thus suggest that the β-turn conformation at Pro(2)-Tyr(3)/Phe(3) is maintained in both species, with the Cys(4) NH group being involved in formation of a transannular 4→1 hydrogen bond.

The 67.89-MHz ^{13}C NMR spectra of peptide **1** and **2** at 293 and 353 K, in $(CD_3)_2SO$, were also investigated (data not shown). At 293 K sharp resonances are observed and there is no evidence for the population of cis isomers about the Cys(1)-Pro(2) peptide bond. Model building studies also suggest that the hydrogen bond between the Cys(4) NH and

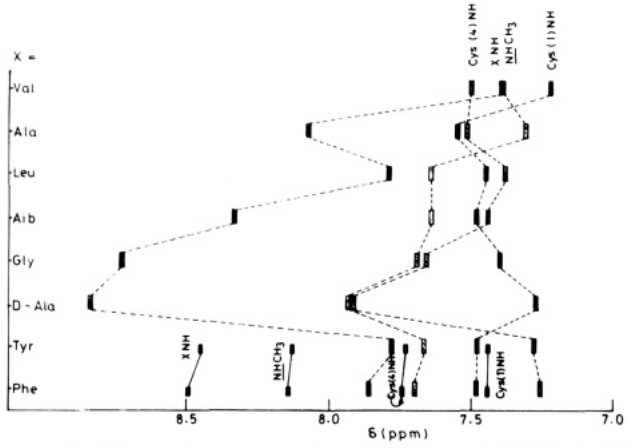

FIGURE 9: Schematic representation of NH chemical shifts in $(CD_3)_2SO$ in eight 14-membered cyclic peptide disulfides with Pro-X intervening sequences.

the Cys(1) CO groups cannot be maintained if the Cys(1)-Pro(2) peptide bond is forced to adopt a cis geometry. Further, the 14-membered disulfide loop is far more constrained for conformations having a Cys(1)-Pro(2) cis peptide bond. For these reasons cis X-Pro conformers are not considered in the subsequent discussion.

^{13}C NMR spectral studies of peptide **1** suggest that heating to 353 K in $(CD_3)_2SO$ results in a selective broadening of certain ^{13}C resonances. For example, the Pro C^{β} (28.6 ppm), Pro C^{γ} (23.5 ppm), and the low-field Pro C^{α} (61.5 ppm) resonances show appreciable broadening. This suggests that the exchange between two species is speeded up at higher temperature, resulting in exchange broadening of these resonances. It would therefore appear that the exchange process largely perturbs the environment of the proline C^{α}, C^{β}, and C^{γ} atoms and one of the other C^{α} atoms (55.7 ppm). The C^{α} resonance at 55.7 ppm may be assigned to the Tyr residue. Similar observations have also been made for the corresponding Pro-Phe analogue, **2**.

Conformations of Peptides **1** *and* **2** *in* $(CD_3)_2SO$. A possible interpretation for the NMR results would involve interconversion between type I and type II β-turn conformations about the Pro(2)-Tyr(3)/Phe(3) segment in peptides **1** and **2**. Figure 9 illustrates the chemical shift correlation diagram for the NH resonances of various 14-membered cyclic peptide disulfides containing Pro-X spacer residues in $(CD_3)_2SO$. The X = Gly or D-Ala peptides have been shown to favor type II β-turn conformations, and these are characterized by extremely low field X NH resonances. In X = Aib peptide both type I and type II β-turn conformations are possible, and evidence for a fast equilibrium has been proposed (Rao et al., 1983). It is of interest to note that the NH of the X resonances (Tyr/Phe in peptides **1** and **2**) of the m conformer in $(CD_3)_2SO$ appears at very low field, suggestive of a type II β-turn structure (Figure 4b). More recently, the solution conformation of *cyclo*-[D-Tyr(Bzl)-Gly-Ile-Leu-Gln-Pro] in $(CD_3)_2SO$ has been reported (Gierasch et al., 1985). Extensive NMR studies have shown that in this peptide the -Pro-D-Tyr(Bzl)- segment adopts a type II β-turn conformation. It is interesting to note that the NH resonance of the D-Tyr(Bzl) residue (X NH) indeed appears at extremely low field in $(CD_3)_2SO$. Steric shielding of the X NH (Tyr/Phe residue) resonance by the aromatic ring may account for the low $d\delta/dT$ values in $(CD_3)_2SO$ in both peptides.

Extensive attempts were made to observe the NOEs characteristic of a type II β-turn conformation, for both peptides **1** and **2** in $(CD_3)_2SO$. However, the magnitudes of NOEs for all sets of protons were exceedingly small. This included conformation-independent NOEs like those between Pro ring protons. This is probably due to unfavorable correlation times in the viscous solvent, $(CD_3)_2SO$ at 293 K (Balaram, 1985; Kartha et al., 1984; Kishore et al., 1985, 1987). Since $C^{\alpha}_{i+1}H - N_{i+2}H$ NOEs are expected only in the minor conformer, small NOE magnitudes make detection of these intensity changes very difficult.

Table III: CD Data on Peptide Disulfides **1** and **2**[a]

	X = Tyr (**1**)		X = Phe (**2**)	
solvent	λ (nm)	$[\theta]_M$	λ (nm)	$[\theta]_M$
$CHCl_3$	277	+4650	284	+3050
	300 (sh)	+2020		
$(CH_3)_2SO$	296	+380	295	+190
	275	−260	268	−310
dioxane	278	+3830	284	+2000
	298 (sh)	+1930		
	228	−38970	226	−32700
CH_3OH–H_2O (1:1)	275	+2900	280	+1230
	295 (sh)	+1200		
	228	−30350	225	−20550
CH_3OH	278	+2440	280	+1300
	296 (sh)	+1200		
	228	−33300	228	−24320
trimethyl phosphate	278	+1200	280	+720
	298 (sh)	+620		
	227	−30950	227	−20500

[a] $[\theta]_M$ is given in units of deg cm^2 dmol^{-1}; sh indicates a shoulder.

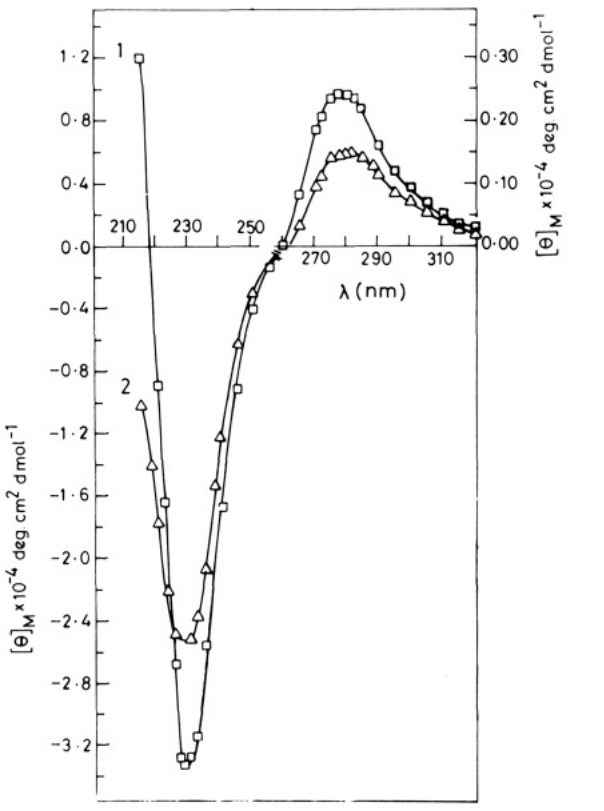

FIGURE 10: CD spectra of peptides **1** and **2** in CH_3OH: (□) **1**; (△) **2**. Peptide concentration was ~1 mg/mL.

CD Studies on Peptides **1** *and* **2**. The CD spectra of peptides **1** and **2** were recorded in CH_3OH, dioxane, TMP, and CH_3OH–H_2O (1:1). The molar ellipticity values are summarized in Table III. Representative CD spectra of peptides **1** and **2** in CH_3OH are shown in Figure 10. The CD spectra of peptides were also recorded in $CHCl_3$ and $(CH_3)_2SO$ in the disulfide region (340–250 nm), in order to evaluate possible

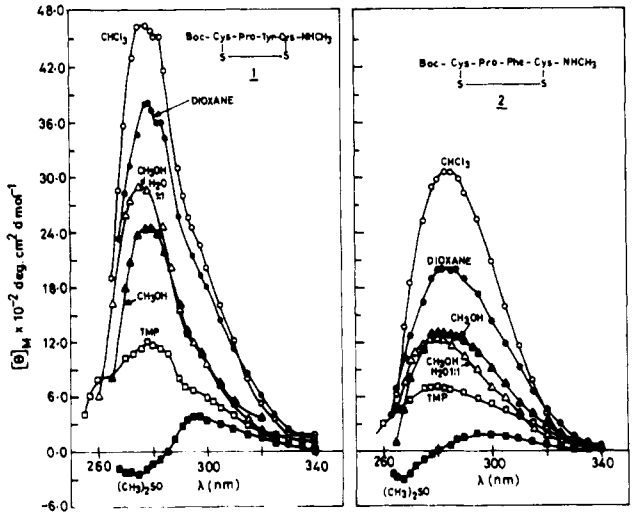

FIGURE 11: Partial CD spectra of peptides **1** (left) and **2** (right) in different solvents: $CHCl_3$ (○); dioxane (●); CH_3OH–H_2O (1:1) (△); CH_3OH (▲); TMP (□); $(CH_3)_2SO$ (■).

changes in the disulfide conformation in these solvents.

The CD spectra of the peptides **1** and **2** in all the solvents studied are characterized by a strong negative band at ~225–230 nm, due to the peptide n–π^* transition. The CD band positions and molar ellipticity values of the n–π^* band are found to be, more or less, independent of solvent polarity in both peptides. This suggests that the peptides **1** and **2** adopt similar, rigid backbone conformations in a variety of solvents. These CD spectra are similar to those reported for model 14-membered cyclic peptide disulfides containing Pro-X sequences (X = Ala, Aib, Leu, Val, Gly, D-Ala). This band is shown to be characteristic of either Pro-X- or X-Pro-containing 14-membered cyclic disulfides, adopting various β-turn structures, stabilized by intramolecular hydrogen bonds (Venkatachalapathi, 1982; Ravi & Balaram, 1983, 1984; Ravi et al., 1983; Rao et al., 1983). It has been noted earlier that in these systems a distinction between type I and type II β-turn conformations may not be readily made from CD data alone (Rao et al., 1983).

Peptide **1** exhibits a band of moderate intensity at 276 nm in $CHCl_3$ (disulfide, n–σ^*). A shoulder at ~300 nm is also observed. The presence of the Tyr residue in this peptide may be expected to contribute to the long-wavelength CD band. A comparison of peptides **1** and **2** facilitates an estimation of this contribution. It is seen from Figure 11 that the long-wavelength shoulder at ~300 nm is indeed absent in **2**, suggesting that this special feature may be due to the phenolic chromophore. The similarity of the CD spectra of peptides **1** and **2** at wavelengths ≤280 nm suggests that the Tyr ring does not make a significant contribution to the observed CD spectra in this region.

From Figure 11 it is clearly seen that, in both peptides **1** and **2**, the band intensity is reduced dramatically in strongly hydrogen bond accepting solvents. Furthermore, in $(CH_3)_2SO$ these peptides exhibit a very weak positive band (297 nm, **1**, +380 deg cm^2 dmol^{-1}; 295 nm, **2**, +190 deg cm^2 dmol^{-1}) and a very weak negative band (275 nm, **1**, −260 deg cm^2 dmol^{-1}; 268 nm, **2**, −300 deg cm^2 dmol^{-1}). A comparison of the disulfide CD bands in $CHCl_3$ and $(CH_3)_2SO$ suggests that conformations about the cystine side chain are dramatically different in these two cases. As noted earlier, two conformations are observed in $(CD_3)_2SO$, by means of ^1H NMR, whereas a single species is seen in $CDCl_3$. The CD results suggest that alterations in backbone conformations are accompanied by changes in disulfide geometry. The solvent-dependent changes in the intensity of the disulfide n–σ^* band suggest that conformations involving different disulfide geometries are populated in solution.

Role of the Aromatic Residue. In $(CD_3)_2SO$ both peptides **1** and **2** exist in two distinct conformations, which are in slow exchange on the NMR time scale. The experimental evidence suggests that the two species correspond to type I (major) and type II (minor) β-turn conformations about the -Pro(2)-X(3)- (X = Tyr or Phe) segment.

The type I–type II β-turn interconversion process formally corresponds to a 180° flip of the peptide bond between the residues $i + 1$ and the $i + 2$ (Figure 4). This process involves a simultaneous reorientation about the C^α–CO (ψ) bond of Pro (type I, ~−30°; type II, ~+120°) and the N–C^α (ϕ) bond of the Tyr(3)/Phe(3) residues (type I, ~−80°; type II, ~+80°). Presumably, such a process involves a correlated rotation about both bonds. The observation of slow exchange on the NMR time scale at room temperature (293 K) implies that the two conformers are separated by an activation barrier of at least 18 kcal/mol. It is of interest to note that relatively high activation barriers have been suggested for rotation about the C^α–CO (ψ) bond in proline peptides. Barriers of ~14 kcal/mol have been estimated in Z-Pro-$NHCH_3$ (Nagaraj et al., 1980) and in the cyclic peptide, *c*-(Pro-Gly)$_2$ (Deber et al., 1974). It is conceivable that, in peptides **1** and **2**, interactions between the aromatic side chain at position 3 and the peptide bond between the residues 2 and 3 can result in a further increase in this rotational barrier. As noted earlier, conformations involving close approach of the aromatic ring and the central peptide unit [between Pro(2) and Tyr/Phe(3)] are indeed energetically favorable (Figure 6), and some evidence for such structures has been obtained from NOE studies in chloroform. It is pertinent to note that such slow conformational interconversions on the NMR time scale, are absent in the case of 14-membered cyclic peptide disulfides having an aliphatic residue (Aib, Leu, Ala, D-Ala, Gly, and Val at position 3).

The occurrence of the L-Tyr or L-Phe residue at the $i + 2$ position of a type II β-turn necessitates ϕ, ψ values in the "D region" of the ϕ, ψ map. An analysis of Tyr residues observed in protein crystal structures establishes that Tyr has a significant tendency to occur in *left-handed* helical conformations, which occur in the region of the conformational map normally allowed for D residues (Robson & Pain, 1971; Finn et al., 1984). A recent theoretical conformational analysis of the biologically active peptide neurotensin yielded a minimum-energy conformation, with the torsion angles ϕ_{Pro} = −63.7°, ψ_{Pro} = +114.5° and ϕ_{Tyr} = +103.6°, ψ_{Tyr} = +87° for the -Pro(10)-Tyr(11)- segment (Finn et al., 1984). Crystal structure analysis of the Phe-containing peptide, cycloamanide A [*cyclo*-(Pro-Val-Phe-Phe-Ala-Gly)] in two polymorphic forms showed that the conformational angles for the L-Phe(4) residue fall in the region characteristic for D residues (Chiang et al., 1982; Karle & Chiang, 1984) (form I, ϕ = +54°, ψ = −118°, and form II, ϕ = +60°, ψ = −122°).

Recent crystal structure determinations of model peptides Piv-Pro-X-$NHCH_3$ (X = L-Phe or L-Tyr) have established type II β-turn conformations in the solid state with ϕ = +64.4°, ψ = +16.3° for L-Tyr residue and ϕ = +62.0°, ψ = +22.8° for L-Phe residue (Aubry et al., 1985). The examples cited above provide strong support that L-Tyr (or L-Phe) residue can indeed adopt the dihedral angles (ϕ, ψ) generally allowed for D residues. Therefore, it would be expected that, in the type II β-turn conformation proposed for the minor conformer in $(CD_3)_2SO$, the positive ϕ, ψ values for the

Tyr(3)/Phe(3) residues may be favored in peptides **1** and **2**. Interestingly, a recent crystal structure determination of Ac-Pro-Phe-Leu·H_2O established a type I β-turn at Pro-Phe with $\phi_{Pro} = -65°$, $\psi_{Pro} = -22°$ and $\phi_{Phe} = -108°$, $\psi_{Phe} = +11°$ (Precigoux et al., 1986). This clearly suggests the likelihood of both type I and type II β-turns at the Pro-Phe segment.

Recently, from the crystal structure analysis of 34 proteins available at 2-Å resolution, the importance of aromatic–aromatic (π–π) interactions in stabilization of protein structure has been reported (Burley & Petsko, 1985). It has also been suggested by these authors that aromatic groups in small peptides can engage in specific, energetically favorable interactions. Such interactions can maintain the peptides in characteristic compact conformations. There is some evidence which suggests that amino acids with aromatic side chains can participate in interactions with carbonyl oxygen atoms in proteins (Burley & Petsko, 1985; Thomas et al., 1982). NMR studies on peptides **1** and **2**, indeed, provide convincing support for the close approach of the aromatic side chain to the peptide bond between Pro(2) and Tyr(3)/Phe(3) residues. It is quite possible that there may be specific, energetically favorable interactions between the aromatic ring and the central and/or C-terminal peptide bond in **1** and **2**. Such interactions are likely to be absent in other Pro-X sequences containing 14-membered cyclic disulfides when the X residue has an aliphatic side chain, i.e., X = Gly, Leu, Ala, Aib, Val, or D-Ala. There are indeed strong evidences for the specific and energetically favorable interactions between the amide and aromatic chromophores in cases of cyclic dipeptides (diketopiperazines) (Thomas et al., 1982). The analysis of experimental results has shown that *c*-(Pro-D-Tyr) and *c*-(Pro-D-Phe), in both polar and nonpolar solvents, assume a common conformer in which the aromatic ring is folded over the diketopiperazine ring. It has been proposed that the folded conformer in aromatic diketopiperazines is stabilized by interactions between the π system of the aromatic ring and the peptide group (Madison et al., 1976; Kopple & Marr, 1967; Vicar et al., 1973; Liwo & Liarkowski, 1985). Polar solvents like water, methanol, and dimethyl sulfoxide seem to favor such folded conformers.

An analysis of the long-wavelength CD band (240–340 nm), which may primarily be assigned to the n–σ^* disulfide band, suggests that significant changes in the geometry about the C^α–C^β–S–S–C^β–C^α of the cystine bridge occur on going from $CHCl_3$ to $(CH_3)_2SO$ (Figure 11). The positive CD band is consistent with a right-handed chirality about the S–S bond (χ_{SS} is positive) with its disulfide dihedral angle of $\sim 90°$ (Linderberg & Michl, 1970; Woody, 1973; Kahn, 1979; Kishore et al., 1987). The dramatic fall in the ellipticities in $(CH_3)_2SO$ suggests the contributions of other conformers, presumably with a left-handed disulfide chirality. Thus, it appears that a conformational change in the disulfide bridge accompanies changes in peptide backbone conformations. Evidence for such conformational coupling has indeed been observed from CD studies of model peptide disulfides (Kishore et al., 1987).

The present studies on peptide models for the glutaredoxin active site provide evidence for conformational variability. While type I β-turn structures are favored in apolar solvents, equilibria between type I and type II β-turns have been suggested in polar solvents like $(CD_3)_2SO$. Specific, energetically favorable interactions between the aromatic side chain and central peptide bond have been invoked to rationalize the high activation barrier to interconversion between type I and type II β-turns. The presence of such a dynamic conformational equilibrium in peptide **1** and its relation to the specific biological function of glutaredoxin remains unclear at present. However, these results in conjunction with earlier studies on thioredoxin models (Ravi & Balaram, 1983) suggest that redox active site disulfide loops adopt highly folded backbone conformations. The maintenance of such structures in the reduced form may facilitate ready reoxidation, while large structural changes on reduction can impede reoxidation. Structural similarities or differences between the oxidized and reduced forms of the active sites may modulate the redox potentials of these systems.

ACKNOWLEDGMENTS

We are grateful to Dr. P. K. C. Paul for providing us with the results of his theoretical calculations and for helping in the preparation of Figure 6.

Registry No. **1**, 112988-34-8; **2**, 112988-35-9.

REFERENCES

Aubry, A., Cung, M. T., & Marraud, M. (1985) *J. Am. Chem. Soc. 107*, 7640–7647.

Balaram, P. (1984) *Proc.—Indian Acad. Sci., Chem. Sci. 93*, 703–717.

Balaram, P. (1985) *Proc.—Indian Acad. Sci., Chem. Sci. 95*, 21–38.

Bax, A., & Lerner, L. (1986) *Science (Washington, D.C.) 232*, 960–967.

Burley, S. K., & Petsko, G. A. (1985) *Science (Washington, D.C.) 229*, 23–28.

Bystrov, V. F., Portnova, S. L., Tsetlin, V. I., Ivanov, V. T. & Ovchinnikov, Yu. A. (1965) *Tetrahedron 25*, 493–515.

Chiang, C. C., Karle, I. L., & Wieland, Th. (1982) *Int. J. Pept. Protein Res. 20*, 414–420.

Deber, C. M., Fossel, E. T., & Blout, E. R. (1974) *J. Am. Chem. Soc. 96*, 4015–4017.

Finn, P. W., Robson, B., & Griffiths, E. C. (1984) *Int. J. Pept. Protein Res. 24*, 407–413.

Gierasch, L. M., Rockwell, A. L., Thompson, K. F., & Briggs, M. S. (1985) *Biopolymers 24*, 117–135.

Hoffmann, R. A., & Forsen, S. (1966) *Prog. Nucl. Magn. Reson. Spectrosc. 1*, 15–204.

Holmgren, A. (1968) *Eur. J. Biochem. 6*, 475–484.

Holmgren, A. (1981) *Curr. Top. Cell. Regul. 19*, 47–76.

Holmgren, A. (1985) *Annu. Rev. Biochem. 54*, 237–271.

Holmgren, A. (1986) in *Thioredoxin and Glutaredoxin Systems: Structure and Function* (Holmgren, A., Branden, C.-I., Jornvall, H., & Sjoberg, B.-M., Eds.) Raven Press, New York.

Holmgren, A., Soderberg, B.-O., Eklund, H., & Branden, C.-I. (1975) *Proc. Natl. Acad. Sci. U.S.A. 72*, 2305–2309.

Hoog, J.-O., Jornvall, H., Holmgren, A., Carlquist, M., & Persson, M. (1984) *Eur. J. Biochem. 136*, 223–232.

Kahn, P. C. (1979) *Methods Enzymol. 61*, 339–376.

Karle, I. L., & Chiang, C. C. (1984) *Acta Crystallogr., Sect. B: Struct. Sci. B39*, 625–637.

Kartha, G., Bhandary, K. K., Kopple, K. D., Go, A., & Zhu, P. P. (1984) *J. Am. Chem. Soc. 106*, 3844–3850.

Kishore, R. (1985) Ph.D. Thesis, Indian Institute of Science.

Kishore, R., Kumar, A., & Balaram, P. (1985) *J. Am. Chem. Soc. 107*, 8019–8023.

Kishore, R., Raghothama, S., & Balaram, P. (1987a) *Biopolymers 26*, 873–888.

Kishore, R., Ishizaki, H., Tu, A. T., Ravi, A., & Balaram, P. (1987b) *Int. J. Pept. Protein Res. 30*, 474–480.

Klintrot, I.-M., Hoog, J.-O., Jornvall, H., Holmgren, A., & Luthman, M. (1984) *Eur. J. Biochem. 144*, 417–423.

Kopple, K. D., & Marr, D. H. (1967) *J. Am. Chem. Soc. 89*, 6193–6200.
Linderberg, J., & Michl, J. (1970) *J. Am. Chem. Soc. 92*, 2619–2625.
Liwo, A., & Ciarkowski, J. (1985) *Tetrahedron Lett. 26*, 1873–1876.
Madison, V., Young, P. E., & Blout, E. R. (1976) *J. Am. Chem. Soc. 98*, 5358–5364.
Meister, A., & Anderson, M. E. (1983) *Annu. Rev. Biochem. 52*, 711–760.
Nagaraj, R., Venkatachalapathi, Y. V., & Balaram, P. (1980) *Int. J. Pept. Protein Res. 16*, 291–298.
Prasad, B. V. V., & Balaram, P. (1984) *CRC Crit. Rev. Biochem. 16*, 307–348.
Precigoux, G., Geoffre, S., & Ourrad, E. (1986) *Acta Crystallogr., Sect. C: Cryst. Struct. Commun. C42*, 721–724.
Rao, B. N. N., Kumar, A., Balaram, H., Ravi, A., & Balaram, P. (1983) *J. Am. Chem. Soc. 105*, 7423–7428.
Ravi, A., & Balaram, P. (1983) *Biochim. Biophys. Acta 745*, 301–309.
Ravi, A., & Balaram, P. (1984) *Tetrahedron 40*, 2577–2583.
Ravi, A., Prasad, B. V. V., & Balaram, P. (1983) *J. Am. Chem. Soc. 105*, 105–109.
Robson, B., & Pain, R. H. (1971) *J. Mol. Biol. 58*, 237–259.
Rose, G. D., Gierasch, L. M., & Smith, J. A. (1985) *Adv. Protein Chem. 37*, 1–109.
Smith, J. A., & Pease, L. G. (1980) *CRC Crit. Rev. Biochem. 8*, 315–399.
Thomas, K. A., Smith, G. M., Thomas, T. B., & Feldman, R. J. (1982) *Proc. Natl. Acad. Sci. U.S.A. 79*, 4843–4847.
Venkatachalapathi, Y. V., Prasad, B. V. V., & Balaram, P. (1982) *Biochemistry 21*, 5502–5509.
Vicar, J., Budesinsky, M., & Blaha, K. (1973) *Collect. Czech. Chem. Commun. 38*, 1940–1956.
Woody, R. W. (1973) *Tetrahedron 29*, 1273–1283.
Wüthrich, K. (1976) in *NMR in Biological Research Peptides and Proteins*, Elsevier/North-Holland, Amsterdam.
Wüthrich, K., Billeter, M., & Braun, W. (1984) *J. Mol. Biol. 180*, 715–740.
Ziegler, D. M. (1985) *Annu. Rev. Biochem. 54*, 305–329.
Zimmerman, S. S., & Scheraga, H. A. (1977) *Biopolymers 16*, 811–843.

Structural Studies of a Folding Intermediate of Bovine Pancreatic Ribonuclease A by Continuous Recycled Flow†

Marc Adler‡ and Harold A. Scheraga*
Baker Laboratory of Chemistry, Cornell University, Ithaca, New York 14853-1301
Received August 18, 1987; Revised Manuscript Received November 5, 1987

ABSTRACT: A new technique, continuous recycled flow (CRF) spectroscopy, has been developed for observing intermediates of any thermally induced, reversible reaction with a half-life of 10 s or longer. The structure can be probed by any spectroscopic method which does not perturb the system. Prolonged signal acquisitions of 8 h for ribonuclease A are possible. CRF was used to investigate the structure of the slow-folding intermediates of chemically intact ribonuclease A (RNase A) during thermal unfolding/folding under acidic conditions. The following conclusions were reached on the basis of the proton nuclear magnetic resonance and far-ultraviolet circular dichroism spectra of a folding intermediate(s): (A) The conformation of the detected folding intermediate(s) is similar to that of the heat-denatured protein. There is only limited formation of new structures. (B) The N-terminal α-helix is partially stable under these conditions and is in rapid (<10 ms) equilibrium with the denatured conformation. (C) There are long-range interactions between the hydrophobic residues of the N-terminal α-helix and the rest of the protein. These interactions persist well above the melting point. (D) An aliphatic methyl group reports on the formation of a new structure(s) that lie(s) outside of the N-terminal region. (E) The structures detected in chemically modified, nonfolding forms of the RNase A are also present in the folding intermediate(s). There are, however, additional interactions that are unique to chemically intact RNase A.

Bovine pancreatic ribonuclease A (RNase A)[1] is a small digestive protein of 124 amino acids that is denatured reversibly by a variety of agents such as chemical denaturants (Garel & Baldwin, 1973; Garel et al., 1976; Schmid & Blaschek, 1981; Lin & Brandts, 1983a; Mui et al., 1985; Schmid et al., 1986) and heat (Harrington & Schellman, 1956; Hermans & Scheraga, 1961). The protein refolds spontaneously when it is returned to conditions that favor the native structure. The process must be more directed than a random sampling of all possible structures since there are too many structures to be sampled in a reasonable amount of time (Wetlaufer, 1973). Presumably, the folding is guided by the formation of local ordered structures involving short- and medium-range interactions.

† This work was supported by research grants from the National Institute of General Medical Sciences (GM-24893) and from the National Science Foundation (DMB84-01811).
‡ NIH postdoctoral fellow, 1987.

[1] Abbreviations: C-peptide, the 13 N-terminal residues of ribonuclease A; CRF, continuous recycled flow; DSS, sodium 2,2-dimethyl-2-silapentane-5-sulfonate; HPLC, high-performance liquid chromatography; N-terminal α-helix, the first α-helix in ribonuclease A which extends from residues 3 to 13; NMR, nuclear magnetic resonance; ppm, parts per million; RNase A, bovine pancreatic ribonuclease A; S-peptide, the 20 N-terminal residues of ribonuclease A; SDS–PAGE, sodium dodecyl sulfate–polyacrylamide gel electrophoresis; $8SO_3^{2-}$-RNase A, disulfide-reduced and sulfonated bovine pancreatic ribonuclease A; T_m, midpoint of the ribonuclease unfolding transition; U_f and U_s, fast- and slow-refolding forms of unfolded ribonuclease A, respectively; UV, ultraviolet; UVCD, ultraviolet circular dichroism; 1D, one dimensional.

0006-2960/88/0427-2471$01.50/0